NASA TECHNICAL NOTE

NASA TN D-6563

NASA TN D-6563

DESIGN STUDY OF SHAFT FACE SEAL WITH SELF-ACTING LIFT AUGMENTATION

V — Performance in Simulated Gas Turbine Engine Operation

by Lawrence P. Ludwig and Robert L. Johnson

Lewis Research Center
Cleveland, Ohio 44135

NATIONAL AERONAUTICS AND SPACE ADMINISTRATION • WASHINGTON, D. C. • DECEMBER 1971

1. Report No.	2. Government Accession No.	3. Recipient's Catalog No.
NASA TN D-6563		

4. Title and Subtitle	5. Report Date
DESIGN STUDY OF SHAFT FACE SEAL WITH SELF-ACTING LIFT AUGMENTATION. V - PERFORMANCE IN SIMULATED GAS TURBINE ENGINE OPERATION	December 1971
	6. Performing Organization Code
7. Author(s)	8. Performing Organization Report No.
Lawrence P. Ludwig and Robert L. Johnson	E-6312
	10. Work Unit No.
9. Performing Organization Name and Address	132-15
Lewis Research Center National Aeronautics and Space Administration Cleveland, Ohio 44135	11. Contract or Grant No.
	13. Type of Report and Period Covered
12. Sponsoring Agency Name and Address	Technical Note
National Aeronautics and Space Administration Washington, D.C. 20546	14. Sponsoring Agency Code

15. Supplementary Notes

16. Abstract

The feasibility and the noncontact operation of the self-acting seal was demonstrated over a range of simulated gas turbine engine conditions from 61 to 152 m/sec (200 to 500 ft/sec) sliding speed. Sealed pressure differentials were 35 to 207 N/cm^2 (50 to 300 psi), and sealed temperatures were 339 to 922 K (150° to 1200° F). Low leakage (about 1/10 that of conventional labyrinth seals) was exhibited in two endurance runs (200 and 338 hr) at 122 m/sec (400 ft/sec), 138 N/cm^2 (200 psi) and 811 K (1000° F) (gas temperature). For these endurance runs, the self-acting pad wear was less than 3.8 micrometers (0.00015 in.); this low wear was attributed to the noncontact operation of the primary seal. Operating problems identified were fretting wear of the secondary seal and erosion of the primary seal by hard particles.

17. Key Words (Suggested by Author(s))	18. Distribution Statement
Gas turbine shaft seals, Face seals, Self-acting seals, Fluid-film seals, Gas seals	Unclassified - unlimited

19. Security Classif. (of this report)	20. Security Classif. (of this page)	21. No. of Pages	22. Price*
Unclassified	Unclassified	20	$3.00

* For sale by the National Technical Information Service, Springfield, Virginia 22151

DESIGN STUDY OF SHAFT FACE SEAL WITH SELF-ACTING LIFT AUGMENTATION

V - PERFORMANCE IN SIMULATED GAS TURBINE ENGINE OPERATION

by Lawrence P. Ludwig and Robert L. Johnson

Lewis Research Center

SUMMARY

A self-acting face seal designed for gas turbine engines was subjected to simulated gas turbine engine operation. This self-acting seal had pads that lifted the primary seal ring out of rubbing contact. Therefore, the seal has high-speed and low-wear potential. The feasibility and noncontact operation of the self-acting seal were demonstrated over a range of operation that included seal sliding speeds of 61 to 152 meters per second (200 to 500 ft/sec), sealed pressure differential of 35 to 207 N/cm^2 (50 to 300 psi), and sealed air temperatures of 339 to 922 K (150° to 1200° F).

The seal was also subjected to endurance runs of 200 and 320 hours at a sliding speed of 122 meters per second (400 ft/sec), a sealed pressure differential of 138 N/cm^2 (200 psi), and a sealed gas temperature of 811 K (1000° F). Air leakage rates were between 0.28 and 0.59 standard cubic meters per minute (10 and 21 scfm); these rates are about 1/10 that of labyrinth seal leakage. Wear of the self-acting pads was less than 3.8 micrometers (0.00015 in.). Finally, the seal was subjected to 40 starts and stops in order to check wear effect due to rubbing contact during starting and stopping. The wear was less than 2 micrometers (0.0001 in.).

The operating problems identified were (a) fretting wear of the secondary sealing ring and (b) primary seal erosion by hard particles carried by the leakage flow.

INTRODUCTION

Shaft seals are used in gas turbine engines to restrict gas leakage into the bearing compartments (sumps). (The number of bearings varies with design: some aircraft engines have seven bearings; others only three.) The types of seals used also varies with engine designs. Some high-bypass-ratio engines for subsonic aircraft use labyrinth seals at the sump locations. Labyrinth seals have high gas leakage rates but have long

lives and high-speed capability. Other engines have rubbing contact (circumferential and face) seals. And as pointed out in reference 1, these contact seals are limited (due to the rubbing contact) in speed, pressure, temperature, and life capability.

Recent studies (refs. 1 to 3) show that face seals with self-acting lift pads operate without rubbing contact. Therefore, these self-acting seals should have long life with speed, pressure, and temperature capabilities greater than conventional rubbing contact seals. Further, because of the small operating film thicknesses (ref. 1), the leakage should be about 1/10 that of labyrinth seals. The self-acting seal is similar in appearance to the conventional face seal; one fundamental difference is the use of self-acting lift pads on the sealing face. Other construction differences of a self-acting seal (fig. 1) are described in reference 4 (a companion report). Two other reports of this series (refs. 5 and 6) give the analysis of the self-acting geometry and the sealing dam. Part IV of this series of reports (ref. 7) presents the seal force balance (for simulated gas turbine engine operation conditions) and resulting operating film thicknesses.

The self-acting seal was tested under simulated gas turbine engine operation and the objectives of these tests were to (1) experimentally confirm the feasibility of using a self-acting seal in a gas turbine engine application, (2) determine leakage rates under sim-

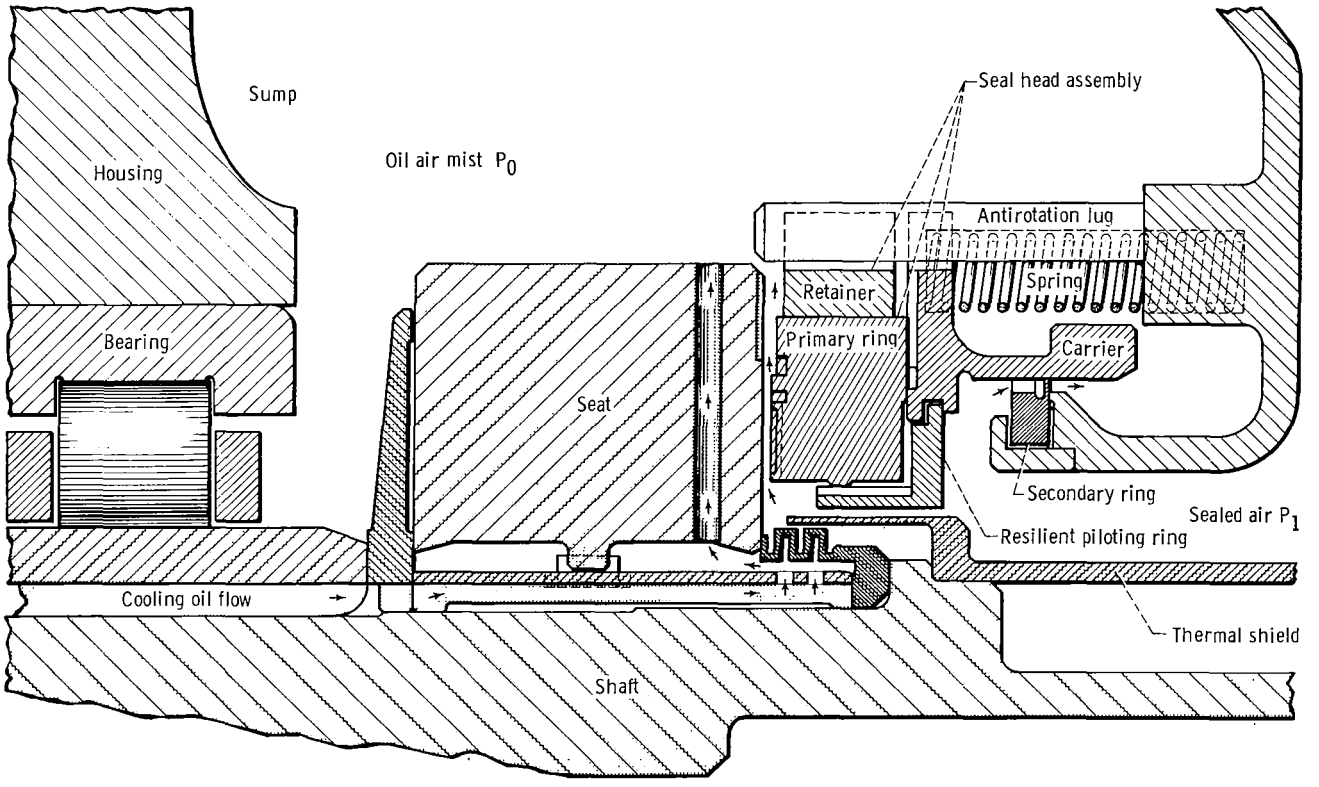

Figure 1. - Shaft face seal with self-acting geometry.

ulated gas turbine engine operating conditions, (3) determine seal operating problems such as wear.

The seal was evaluated in a rig that simulated an engine sump. The mean seal diameter of 16.76 centimeters (6.60 in.) is typical of some engine seals. In order to show capability, the seals were operated at a 152-meter-per-second (500-ft/sec) sliding velocity, a 207-N/cm^2 (300-psi) sealed pressure differential, and a 922 K (1200° F) sealed gas temperature. (These operating conditions far exceed the capability of conventional face seals in aircraft engines.) Current capability of the conventional face seal is approximately 107 meters per second (350 ft/sec), 86 N/cm^2 (125 psi), and 728 K (850° F) (ref. 3). The range of operating conditions covered those expected in aircraft engine operation. The seal was designed at the Lewis Research Center, and the experimental work was performed by Pratt and Whitney Aircraft under NASA contract NAS-3-7609 (ref. 8).

APPARATUS AND PROCEDURE

Test Rig

Figure 2 is a cross-sectional view of the rig used to simulate the environment of a bearing compartment (sump) in a gas turbine engine. The rig shaft was mounted on a 130-millimeter-bore roller bearing and on a 110-millimeter-bore duplex ball bearing that carried the thrust from the sealed pressure. Both bearings are typical of those used in large aircraft engines. The air to be sealed (maximum of 922 K (1200° F) and 207 N/cm^2 (300 psi)) is introduced through tubes as shown in figure 2. Thus, the sealed pressure is at the inside diameter of the primary ring, and air leakage is across the primary sealing faces (dam) into the bearing sump (also see fig. 1). Air also leaks

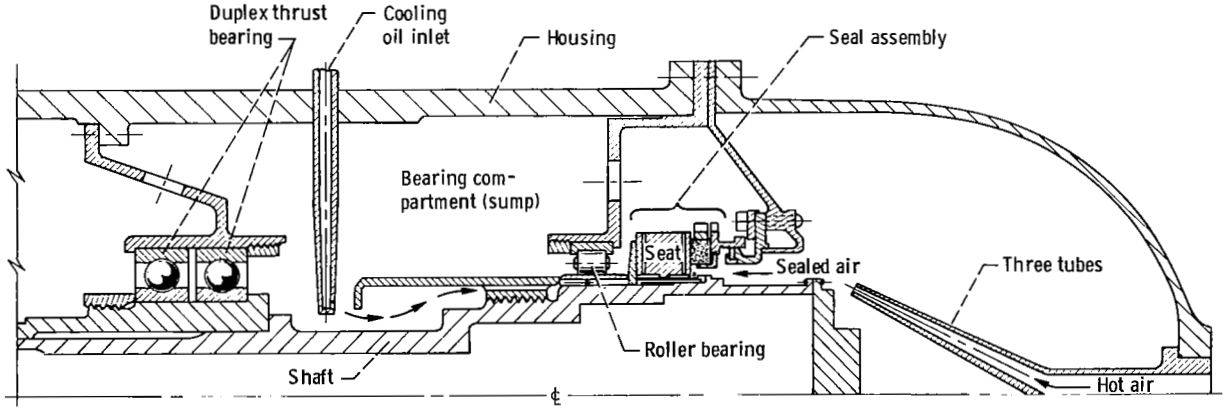

Figure 2. - Rig used for experimental evaluation of seals.

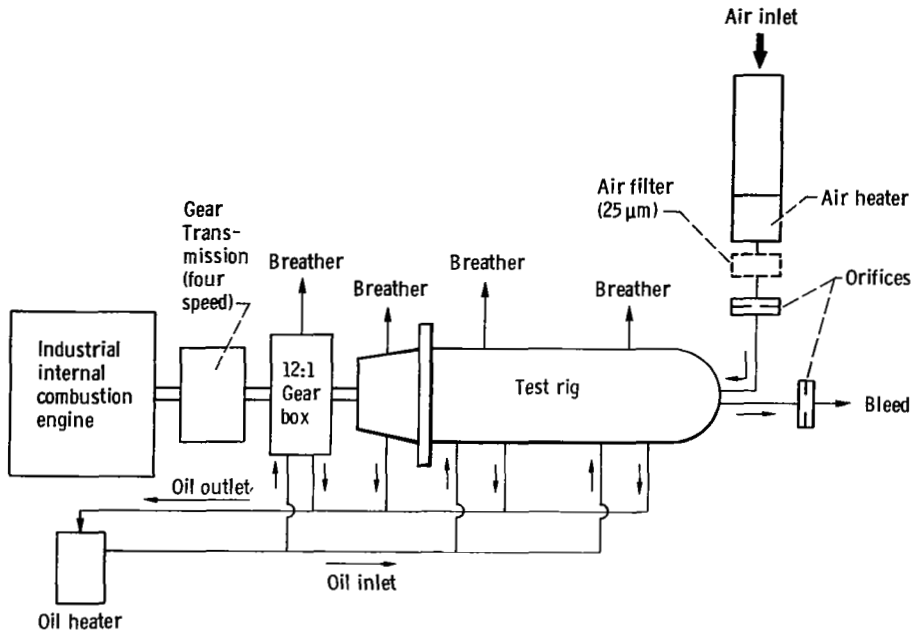

Figure 3. - Test facilities.

across the secondary sealing surfaces into the sump.

The test rig is driven by an industrial internal combustion engine driving through a four-speed truck transmission and 12:1 step-up gear box (fig. 3). The operating speed range was 7000 to 17 500 rpm. Oil was supplied to the rig bearing at temperatures typical of engine sumps (394 K (250^{o} F) to 450 K (350^{o} F)). The sealed air is heated to operating temperature by a resistance heater placed in the system as depicted in figure 3. In the later runs a 25-micrometer filter was introduced (shown dashed in fig. 3) for the purpose of reducing the amount of hard particles carried by the air leakage flow. (The hard particles are probably oxides generated in the resistance heater.)

Test Seals

The test seal is shown in figure 1 and is described in detail in a companion paper in reference 4. Seal nomenclature is given in figure 4. The principal components are (1) the seat (rotating portion), (2) the primary ring assembly (nonrotating but movable axially), and (3) the secondary ring (nonrotating).

Molybdenum alloy (TZM) was selected for the seat material since its high conductivity and low thermal expansion provides lower thermal deformation than conventional seat materials. For a discussion on the effect of thermal deformation on seal perform-

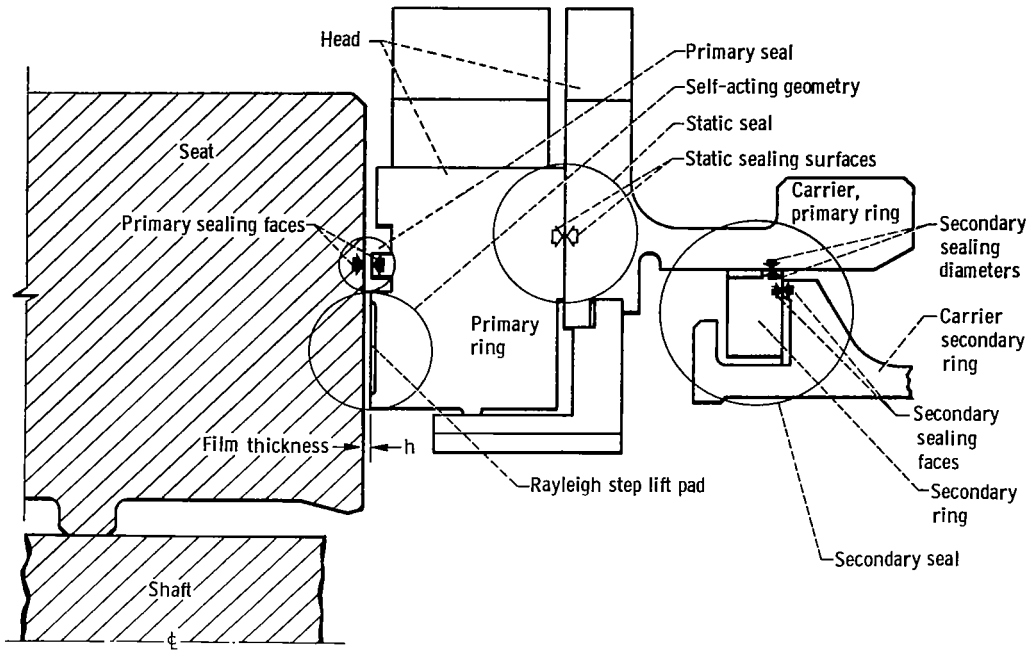

Figure 4. - Seal nomenclature for self-acting face seal.

ance see references 10 and 11. The seat is mounted over its centroid and on a shaft spacer with radial flexibility. This mounting mitigates the effects of shaft thermal movement that would deform the seat face (and, hence, affect seal force balance (ref. 1)). The seat is axially clamped through a bellows that limits the clamping force to approximately 8896 newtons (2000 lbf); therefore, seat deformation due to clamping forces are mitigated. Cooling oil passing through 45 radial holes that are drilled near the sealing face minimize thermal deformation (see ref. 4 for details). The outer portion of the seat face contains spiral grooves that pump back any oil tending to leak toward the sealing dam. (An oil film in the primary seal is undesirable since oil film shearing would generate heat and cause thermal deformation.) A chromium carbide coating on the seat face provides wear and oxidation resistance.

The head assembly consists of three parts. A primary ring (carbon), which has an interference fit in a retaining ring (TZM material), and a carrier, which carries the closing springs and pilots the secondary ring (piston ring). Note that a static seal is formed by the lapped surfaces of the primary ring (carbon) and the carrier. Three antirotation lugs provide radial location for the carrier and the retaining ring. Concentricity between the carrier and primary ring sealing diameters is maintained by a resilient piloting ring. The sealing face of the carbon contains the self-acting lift pads and the sealing dam (fig. 5). These are discussed in detail in references 5 and 6.

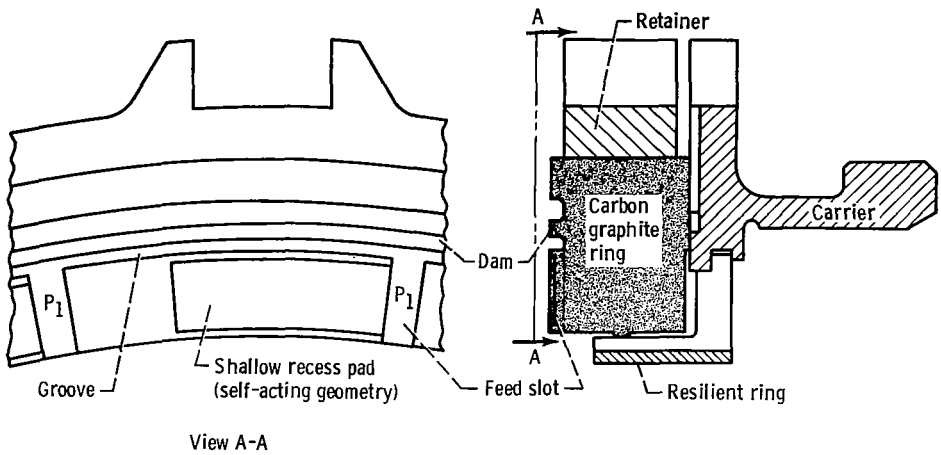

Figure 5. - Self-acting seal with pads on primary ring.

Seal Inspections

Inspections of seal flatness were made by light interference techniques before and after the runs. Frequent visual inspection during the test runs provided a check for seal wear, oil leakage, and oxidation. Seal wear was accurately determined by surface profile traces. Seal leakage checks at 0 rpm, before and after operation, provided additional checks on seal condition. For example, the amount of wear of the secondary and primary seal wear could be determined qualitatively by the static leakage checks.

RESULTS AND DISCUSSION

Preliminary Dynamic Checkout

This checkout was run to determine if the seal rig and seal were functioning properly. Gas leakage measurements through the seal were made before and after test runs. Gas leakage measurements during the test runs were an indicator of seal operating film thickness. These were compared with the predicted values (ref. 6) as a check on proper operation. Cooling oil temperature was 394 K (250° F). Seal sliding speeds were 61, 91, 107, and 122 meters per second (200, 300, 350, and 400 ft/sec), and seal pressure differentials ranged from 35 to 138 N/cm^2 (50 to 200 psi). In all cases the sealed air temperature was near 339 K (150° F).

Figure 6 shows that the seal leakages are speed dependent. The increase in leakage with increasing speed is due in part, to the greater gas film thicknesses developed at the higher speeds by the self-acting geometry. (The other reason for the increase is asso-

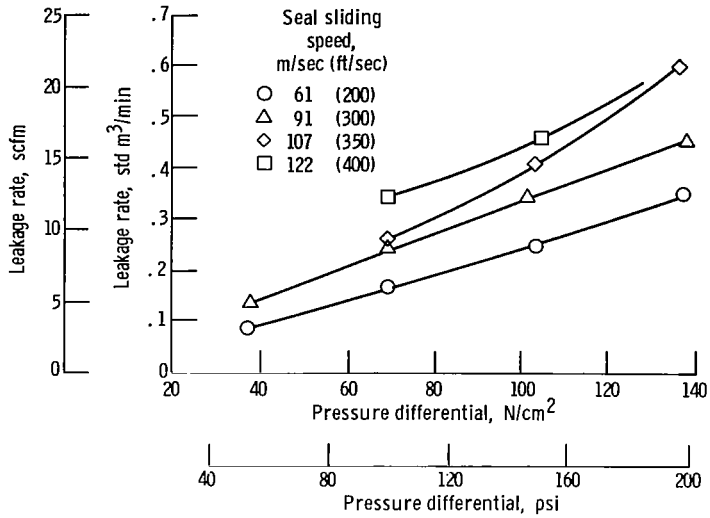

Figure 6. - Air leakage pass primary seal, sealed air temperature, 339 K (150° F).

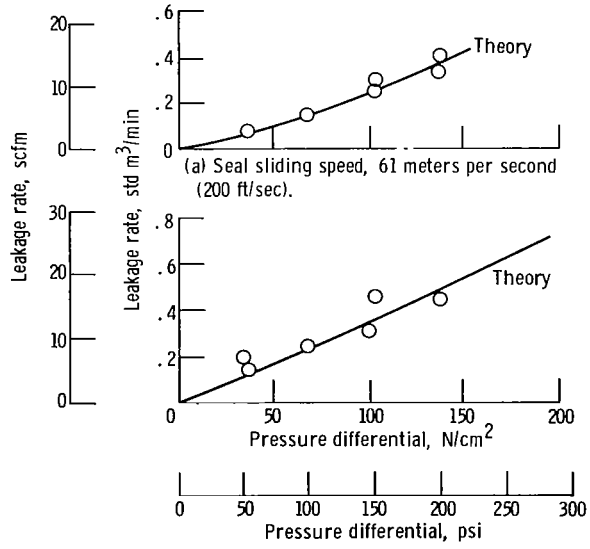

(a) Seal sliding speed, 61 meters per second (200 ft/sec).

(b) Seal sliding speed, 91 meters per second (300 ft/sec).

Figure 7. - Air leakage pass primary seal; sealed air temperature, 339 K (150° F).

ciated with the response of the primary ring to the run out of the seat face. This is discussed in ref. 9.)

As would be expected the primary seal leakage increases with sealed pressure increase, and this is shown in figure 7 for operation at 61 and 91 meters per second (200 and 300 ft/sec) sliding velocity. (The gas leakage past the secondary seal was determined in a separate static fixture and substracted from the total leakage to get net leakage pass the primary seal.)

Simulated Engine Operation

These runs simulated the environment of a gas turbine engine sump over a wide range of combinations of oil temperature, seal sliding speed, sealed pressure differential, and sealed air temperature. Table I shows a matrix of 36 operating points for which seal leakage was measured both for cooling oil temperature of 394 K (250^{o} F) and for 450 K (350^{o} F). The running time at each operating point was a minimum of 15 minutes, which was long enough to reach equilibrium conditions. A general increase in air leakage with increasing speed is evident. Also, as previously mentioned, the air leakage increases with increasing sealed pressure differentials. During the operation (not recorded in table I), it was observed that increasing the oil temperature with all other parameters constant did lower the seal leakage rates slightly. This was attributed to slight changes in seal deformation and to increases in leakage air temperature that accompany the changes in oil-in temperature. Although, as shown in figure 8, an increase in the sealed air temperature had no appreciable effect on leakage at 91 and 107 meters per second (300 and 350 ft/sec). However, there is a pronounced anomaly at 122 meters per second (400 ft/sec) and 589 K (600^{o} F). From a theoretical standpoint, the leakage should decrease as temperature increases because of the associated increase in air viscosity. However, other competing factors such as face deformation can offset the temperature effect.

Endurance Runs

Endurance runs to 338 hours were made for the purpose of checking long-term effects such as carbon oxidation and dirt erosion. For these runs, various operating conditions were used, but the majority of operation was at a 112 meter-per-second (400-ft/sec) sliding speed, a 138-N/cm^{2} (200-psi) sealed pressure differential, and a 800 K (1000^{o} F) sealed air temperature. Seal leakage was monitored during these runs.

The seal was first subjected to a 50-hour endurance run at a sliding velocity of 122

TABLE I. - AIR LEAKAGE RATES DURING SIMULATED ENGINE OPERATION

Oil inlet temperature		Seal sliding speed		Seal pressure differential		Air temperatures, K (°F)							
						478 (400)		589 (600)		700 (800)		811 (1000)	
						Air leakage rates							
K	°F	m/sec	ft/sec	N/cm^2	psi	std m^3/min	scfm	std m^3/min	scfm	std m^3/min	scfm	std m^3/min	scfm
394	250	91	300	69	100	0.42	14.8	0.46	16.3	0.42	14.7	0.48	16.9
				103	150	.59	21.0	.59	20.9	.55	19.4	.67	23.6
				138	200	.72	25.5	.90	31.8	.82	28.9	.77	27.2
		107	350	69	100	0.47	16.7	0.52	18.2	0.50	17.6	0.50	17.5
				103	150	.66	23.2	.72	25.3	.75	26.6	.70	24.8
				138	200	.72	25.5	.65	22.8	1.00	35.5	.91	32.1
		122	400	69	100	0.34	12.0	0.82	29.0	0.82	28.8	0.76	26.9
				103	150	.66	23.3	1.08	38.0	.95	33.5	.93	32.8
				138	200	.91	32.1	1.37	48.5	1.18	41.6	1.10	39.0
450	350	91	300	69	100	0.55	19.3	0.39	13.8	0.38	13.3	0.35	12.3
				103	150	.61	21.5	.69	24.4	.55	19.3	.50	17.8
				138	200	.77	27.2	.85	30.2	.73	25.9	.67	23.6
		107	350	69	100	0.61	21.6	0.49	17.2	0.43	15.2	0.43	15.1
				103	150	.63	22.4	.71	25.0	.62	21.8	.55	19.1
				138	200	.76	26.8	.84	30.9	.79	27.9	.76	26.8
		122	400	69	100	0.62	22.0	0.82	29.0	0.68	24.0	0.75	26.5
				103	150	.74	26.2	.86	30.2	.86	30.2	.95	33.5
				138	200	.84	29.6	1.15	40.5	1.08	38.2	.76	27.0

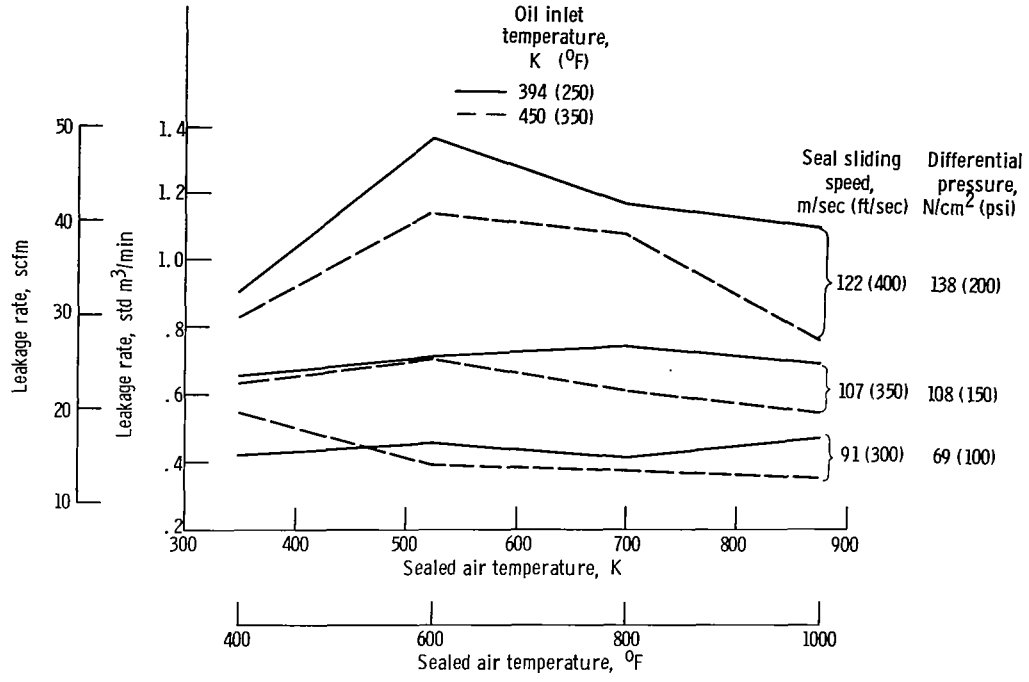

Figure 8. - Air leakage rates during simulated engine operation.

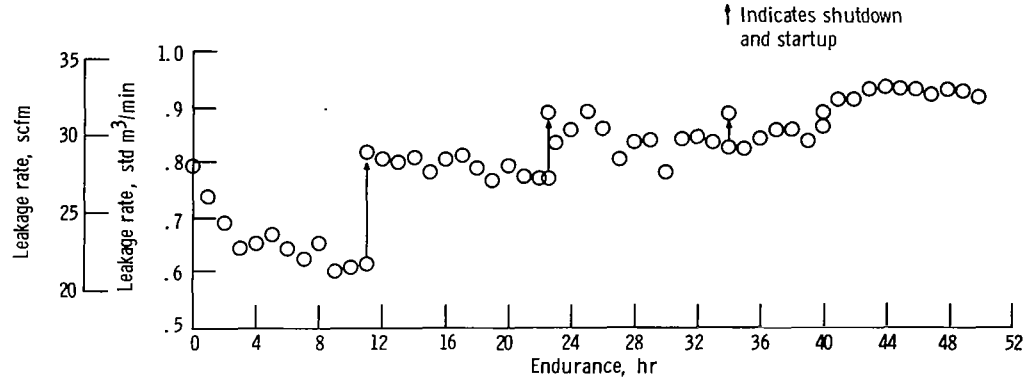

Figure 9. - Air leakage of self-acting seal during 50-hour endurance run. Seal sliding speed, 122 meters per second (400 ft/sec); seal pressure differential, 138 N/cm^2 (200 psi); sealed air temperature, 811 K (1000° F).

meters per second (400 ft/sec), a pressure differential of 138 N/cm^2 (200 psi), and an air temperature of 811 K (1000° F). The oil inlet temperature was 350° F (450 K). During the 50 hours, the seal leakage progressively increased as shown in figure 9 (the increase was attributed to slight erosion of the primary seal), the seal was frequently removed for visual inspection, and six starts and stops were made. Further, the seal was subjected to drive shaft vibration that required rig shutdown and repair. Inspection during and after the 50 hours showed that the self-acting land area was being progressively polished from outer edge toward the inner edge. Also, it was noted that the primary ring sealing face (dam) area became scratched (eroded) as testing progressed. These scratches were caused by hard oxide particles generated in the air heater and carried

with the air leakage. The general appearance of the sealing faces was very satisfactory, with the wear of the self-acting pads less than 2 micrometers (0.0001 in.). This low wear indicates that the seal is operating with positive separation of the surfaces.

The same seal was then subjected to a 100-hour continuous (except for drive engine failure) run at a sliding speed of 122 meters per second (400 ft/sec), a sealed pressure differential of 138 N/cm^2 (200 psi), and a gas temperature of 811 K (1000° F). From an initial seal leakage of 1.13 standard cubic meters per minute (40 scfm), the seal leakage decreased (see fig. 10) to 0.79 standard cubic meters per minute (28 scfm) at the end of the 100 hours (total time 150 hr). The cause of this gradual leakage decrease was not determined. However, it may have been caused by better sealing of the secondary ring (wear-in process).

Inspection revealed that the chromium-carbide-coated molybdenum seat was in excellent condition with no sign of severe contact between the seat and the nosepiece. The self-acting pad land surfaces were polished, and the primary ring sealing face (dam) had circumferential scratches indicating further erosion due to air entrained debris. This erosion or scratching is shown in figure 11, which is a surface profile trace across a self-acting pad and the sealing dam. Traces before and after the 150 hours total running show that erosion 38 micrometers (0.0015 in.) deep had occurred near the inner diameter of the sealing dam (fig. 11(b)). The location and shape of the wear area rules out thermal deformation as a cause of contact and wear. The profile traces (before and after the test) of the self-acting recess depth reveal that the wear of the self-acting pads was 1.5 micrometers (0.00006 in.).

The final 50-hour endurance run was made at a sliding speed of 76 meters per second (250 ft/sec), a pressure differential of 69 N/cm^2 (100 psi), and a air temperature of 700 K (800° F). The air leakage started at 0.38 standard cubic meter per minute (13.5 scfm) (fig. 12) and remained essentially constant for the 50 hours. A rig power failure at 44 hours into the run shut the rig down but did not alter the seal performance. Surface profile traces (fig. 13) taken after the 50-hour run (200 total hr) reveal that the pad wear

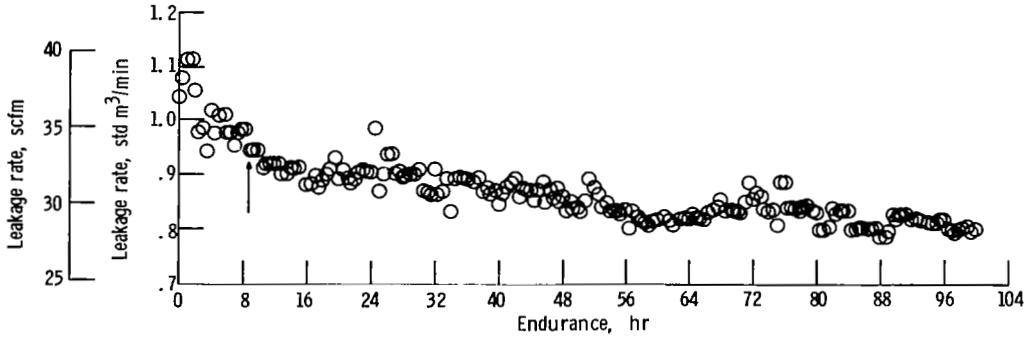

Figure 10. - Air leakage self-acting seal during 100-hour endurance run. Seal sliding speed, 122 meters per second (400 ft/sec); sealed pressure differential, 138 N/cm^2 (200 psi); sealed gas temperature, 811 K (1000° F).

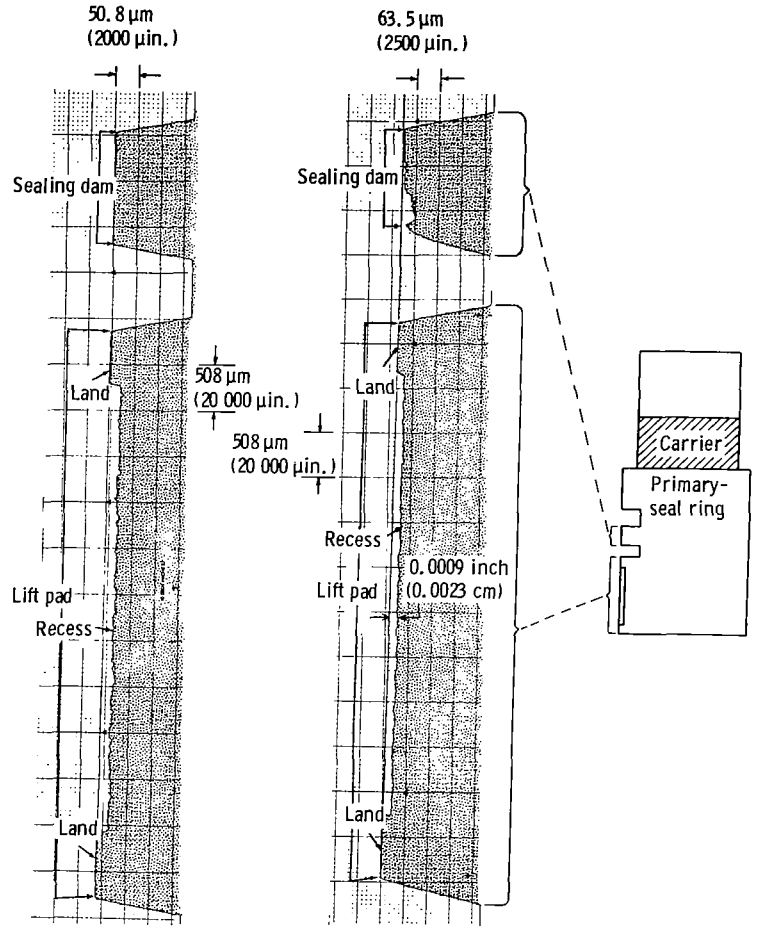

(a) Before 150-hour run. (b) After 150-hour run.

Figure 11. - Surface profile traces across self-acting pad and sealing dam before and after 150 hours of endurance running. Seal sliding speed 122 meters per second (400 ft/sec); sealed pressure differential, 138 N/cm^2 (200 psi); sealed gas temperature 811 K (1000^0 F).

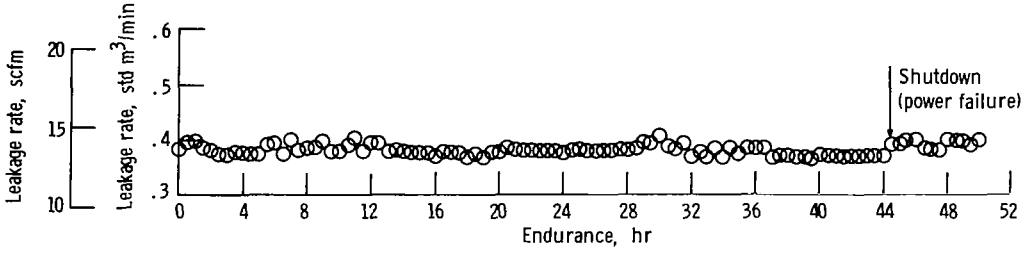

Figure 12. - Air leakage 50-hour endurance run; sliding speed, 76 meters per second (250 ft/sec); sealed pressure differential, 69 N/cm^2 (100 psi); sealed gas temperature, 700 K (800^0 F).

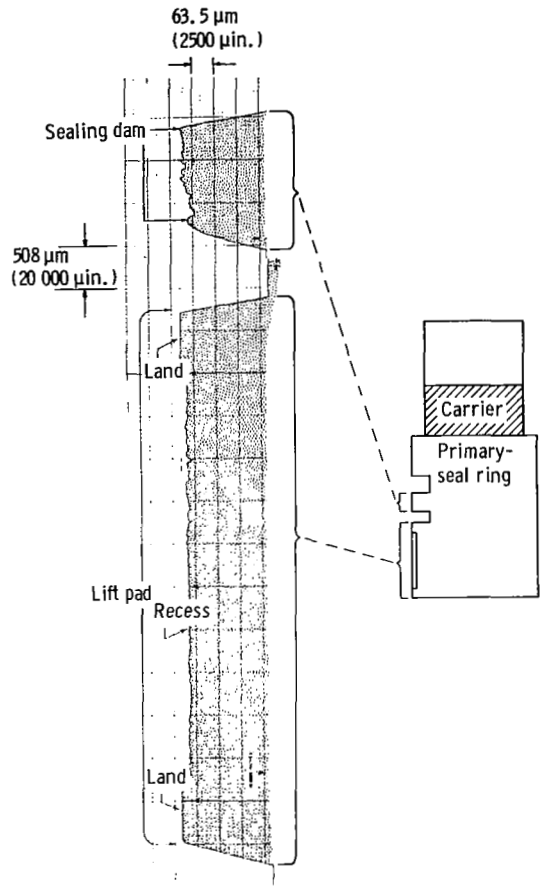

Figure 13. - Surface profile trace radially across lift pad and sealing dam after 200 hours. Sliding speed, 122 meters per second (400 ft/sec); sealed pressure differential, 138 N/cm^2 (200 psi); sealed gas temperature, 811 K (1000^0 F).

was 3.5 micrometers (0.00014 in.) and that the sealing dam scratch depth had increased to 41 micrometers (0.0016 in.).

320-Hour Endurance Run

A 320-hour endurance run was made on a second seal. This run consisted of a 120-hour segment and a 200-hour segment. The operating condition for the entire 320 hours was a 122-meter-per-second (400-ft/sec) sliding speed, a 200-pound-per-square-inch (138-N/cm^2) sealed pressure differential, and a 1000^0 F (811 K) sealed air temperature.

The air leakage during the first 120-hour segment (see fig. 14) averaged about 0.33 standard cubic meter per minute (11.7 scfm). The sharp increase in leakage at 116 hours was caused by failure of the thrust bearing. (Bearing spall produced severe rig

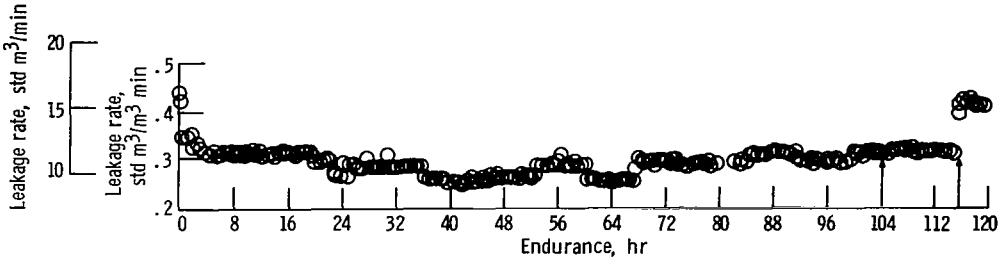

Figure 14. - Air leakage for 120-hour endurance run. Sliding speed, 122 meters per second (400 ft/ sec); sealed pressure differential, 138 N/cm^2 (200 psi); sealed air temperature, 811 K (1000^0 F). Note: The increase in leakage at 116 hours was caused by vibration that resulted from bearing failure.

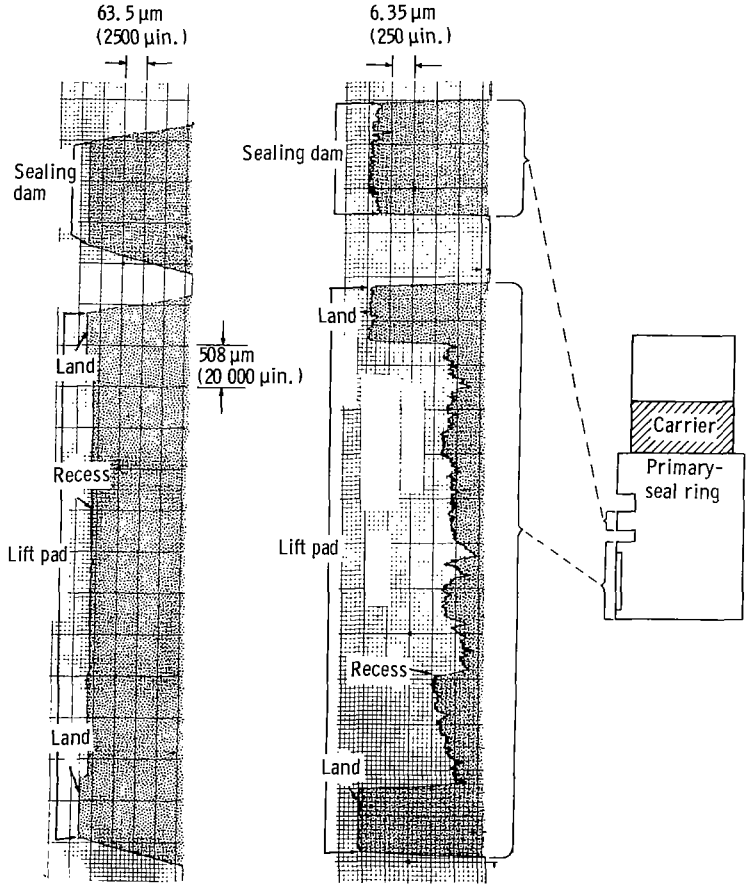

(a) Before 120-hour endurance run.

(b) After 120-hour endurance run.

Figure 15. - Surface profile trace radially across lift pad and sealing dam. Sliding speed, 122 meters per second (400 ft/sec); sealed pressure differential, 138 N/cm^2 (200 psi); sealed gas temperature, 811 K (1000^0 F).

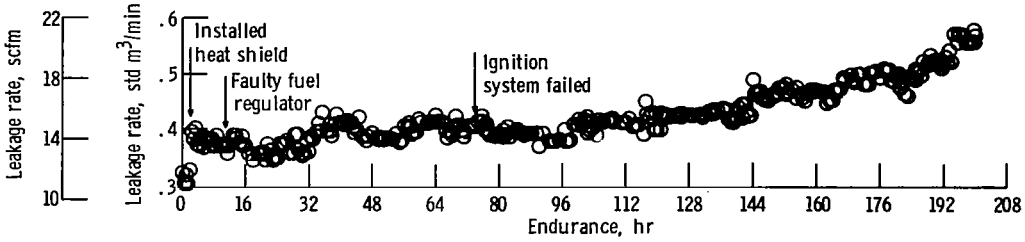

Figure 16. - Air leakage during 200 hours of endurance running. Sliding speed, 122 meters per second (400 ft/sec); sealed pressure differential, 138 N/cm^2 (200 psi); sealed gas temperature, 811 K (1000^0 F).

vibrations.) The surface profile traces taken before and after the 120-hour endurance run are shown in figure 15. (The vertical scales of the two traces are different.) Inspection revealed that the dam had circumferential scratches as in the previous seal. The deepest scratch was 5 micrometers (0.0002 in.). The average pad wear was 1.27 micrometers (0.00005 in.).

The leakage rate during the 200-hour segment is shown in figure 16. For the first 100 hours, the leakage rate averaged 0.39 standard cubic meter per minute (14 scfm). However, during the last 100 hours, the leakage rate gradually increased to 0.59 standard cubic meter per minute (21 scfm). Since post-test inspection revealed secondary seal wear, this increase in leakage was attributed to fretting of the secondary ring (piston ring) and its mating surface (secondary sealing diameter). As a check on this theory, a static test of the primary ring and secondary ring was compared with that of the primary ring and a new secondary ring mated to an unused portion of the secondary sealing diameter. These checks are shown in table II. Note that the used piston ring contributes significantly to the seal leakage.

Inspection revealed an increase in the number of scratches in the sealing dam (see fig. 17). The deepest scratch depth is 5 micrometers (0.0002 in.), which is the same as after the 120-hour segment. However, the number of shallower scratches has increased. Shutdowns due to driving engine ignition failure and faulty fuel regulator had no adverse

TABLE II. - STATIC CHECK OF SEAL LEAKAGE

Pressure		Used primary ring and used piston ring		Used primary ring and new piston ring	
N/cm^2	psi	Air leakage rates			
		std m^3/min	scfm	std m^3/min	scfm
6.9	10	0.05	1.70	0.02	0.70
13.8	20	.08	3.00	.03	1.20
20.7	30	.12	4.15	.05	1.70

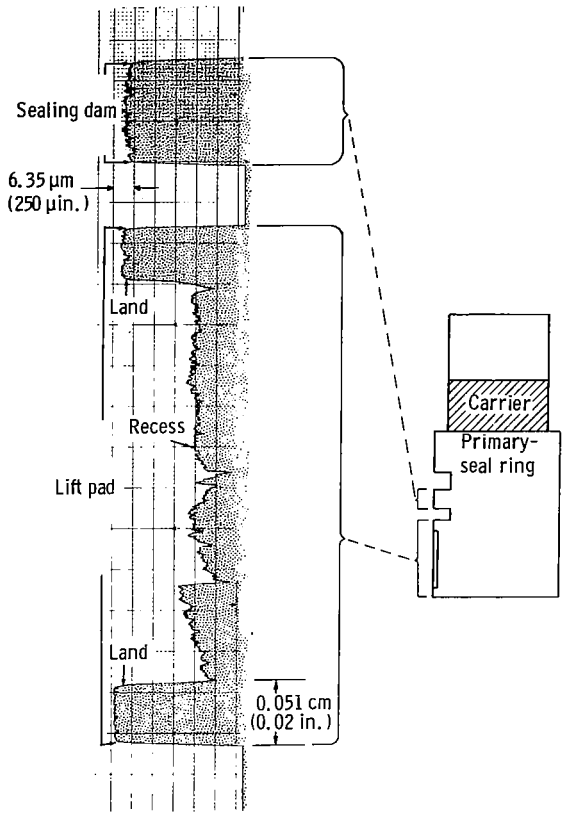

Figure 17. - Surface profile trace radially across lift pad and sealing dam after 200-hours endurance run. Total time on seal, 338 hours; sliding speed, 122 meters per second (400 ft/sec); sealed pressure differential, 138 N/cm^2 (200 psi); sealed gas temperature, 811 K (1000^0 F).

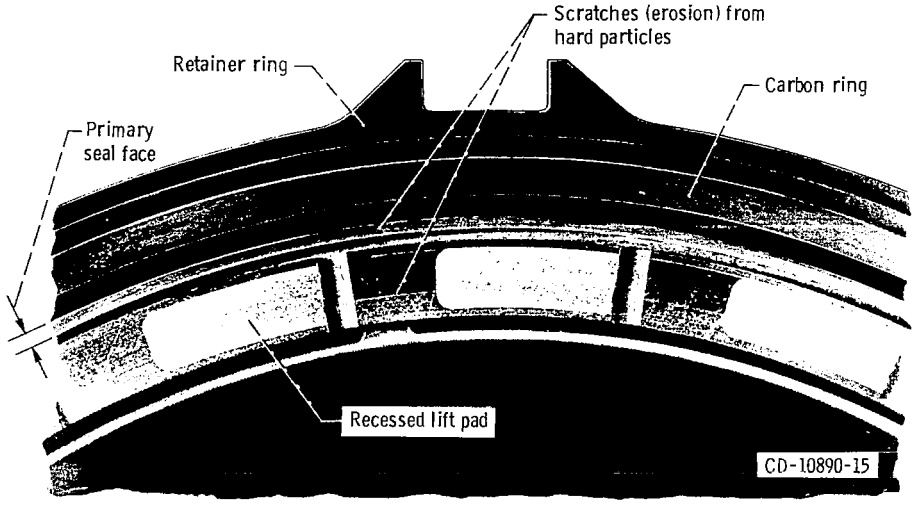

Figure 18. - Primary ring assembly after 320 hours of operation. Sliding speed, 122 meters per second (400 ft/sec); sealed pressure differential, 138 N/cm^2 (200 psi); sealed air temperature, 811 K (1000^0 F).

effect on subsequent seal operation (see fig. 16).

Figure 18 shows the condition of the primary ring after the 320-hour endurance run. Original polishing marks still visible in the surface of the lift pad geometry are evidence that the wear was very small. The several scratches on the lift-pad geometry were attributed to hard debris carried in the air. Note that the sealing dam has a more scratched appearance than the lift pads. Therefore, the majority of the hard particles do not enter the lift-pad region but pass through the feed slots (fig. 5) and then directly across the seal dam.

Wear Due to Starting and Stopping

In order to check the effect of starting and stopping, the seal was subjected to 40 starts and stops. The runs were conducted with room-temperature air at 69 N/cm^2 (100 psi). The seal speed was increased from 0 to 76 meters per second (0 to 250 ft/sec) in about 15 seconds. The seal was then allowed to coast to a stop (required about 25 sec). A comparison of the surface profile traces before and after the 40 starts and stops revealed carbon wear to be less than 1.27 micrometers (0.00005 in.).

Operation at Advanced Conditions

To establish the capability of the seal, it was operated at 137 to 152 meters per second (450 to 500 ft/sec) with pressure to 207 N/cm^2 (300 psi) differential and with sealed temperatures to 922 K (1200° F). The total time at 152 meters per second (500 ft/sec), 922 K (1200 K), and 207 N/cm^2 (300 psi) was 2.7 hours. Leakage was 0.59 standard cubic meter per minute (21 scfm). The total time at 137 to 152 meters per second (450 to 500 ft/sec) was 23 hours; sealed pressures were between 200 and 300 psi (138 and 207 N/cm^2).

The condition of the seal was similar to that shown in figure 18 in that the original polishing marks were still visible; this indicates that the seal operated without rubbing contact at these advanced conditions. Scratching due to hard particles was also evident in the lift-pad lands and across the primary seal face.

SUMMARY OF RESULTS

A self-acting seal designed for gas turbine engines was subjected to simulated operation in an experimental rig that duplicated a gas turbine engine bearing sump. The seal

diameter of 16.76 centimeters (6.60 in.) is typical of some engine seals. The seal was subjected to range of simulated operation that included sliding speeds of 61 to 152 meters per second (200 to 500 ft/sec), sealed pressure differentials of 35 to 207 N/cm^2 (50 to 300 psi), and sealed air temperatures of 339 to 922 K (150° to 1200° F). Furthermore, the seal was subjected to endurance runs up to 320 hours at a 122-meter second (400-ft/sec) sliding speed, 138-N/cm^2 (200-psi) sealed pressure differential, and a 1000° F (811 K) sealed air temperature. Air leakage measurements and seal inspections after running revealed that:

1. The self-acting seal ran without rubbing contact during all of the simulated engine operating conditions and during the endurance runs (which ranged up to 320 hr). Of particular interest was that noncontact operation was maintained at the advanced conditions of a 152-meter-per-second (500-ft/sec) sliding speed, a 207-N/cm^2 (300-psi) sealed pressure differential, and a 1200° F (922 K) sealed air temperature.

2. The leakage rates during simulated engine operation ranged from 0.34 to 1.36 standard cubic meters per minute (12 to 48 scfm). During endurance running the leakage rates ranged from 0.28 to 0.59 standard cubic meter per minute (10 to 21 scfm). These leakage rates are one-tenth that obtained with conventional seal practice.

3. Self-acting seal wear proved to be insignificant and was less than 3.8 centimeters (0.00015 in.) during the endurance runs (320 hr maximum run time).

4. Two seal wear problems were noted. These are (1) fretting wear of the secondary ring (piston ring) and (2) erosion of the seal dam (primary seal) by hard particles.

5. Wear due to starts and stops proved to be insignificant. For 40 starts and stops wear was less than 2 micrometers (0.0001 in.).

Lewis Research Center,
National Aeronautics and Space Administration,
Cleveland, Ohio, September 1, 1971,
132-15.

REFERENCES

1. Johnson, Robert L.; and Ludwig, Lawrence P.: Shaft Face Seal with Self-Acting Lift Augmentation for Advanced Gas Turbine Engines. NASA TN D-5170, 1969.

2. Johnson, Robert L.; Loomis, William R.; and Ludwig, Lawrence P.: Performance and Analysis of Seals for Inerted Lubrication Systems of Turbine Engines. NASA TN D-4761, 1968.

3. Parks, A. J.; McKibben, R. H.; Ng, C. C. W.; and Slayton, R. M.: Development of Main Shaft Seals for Advanced Air Breathing Propulsion Systems. Rep. PWA-3161, Pratt & Whitney Aircraft (NASA CR-72338), Aug. 14, 1967.

4. Ludwig, Lawrence P.; and Johnson, Robert L.: Design Study of Shaft Face Seal with Self-Acting Lift Augmentation. III - Mechanical Components. NASA TN D-6164, 1971.

5. Zuk, John; Ludwig, Lawrence P.; and Johnson, Robert L.: Design Study of Shaft Face Seal with Self-Acting Lift Augmentation. I - Self-Acting Pad Geometry. NASA TN D-5744, 1970.

6. Zuk, John; Ludwig, Lawrence P.; and Johnson, Robert L.: Design Study of Shaft Face Seal with Self-Acting Augmentation. II - Sealing Dam. NASA TN D-7006, 1970.

7. Ludwig, Lawrence P.; Zuk, John; and Johnson, Robert L.: Design Study of Shaft Face Seal with Self-Acting Lift Augmentation. IV - Force Balance. NASA TN D-6568, 1971.

8. Povinelli, V. P.; and McKibben, A. H.: Development of Mainshaft Seals with Advanced Air Breathing Propulsion Systems - Phase II. Rep. PWA-3933, Pratt & Whitney Aircraft (NASA CR-72737), June 23, 1970.

9. Hady, William F.; and Ludwig, Lawrence P.: Experimental Investigation of Self-Acting-Lift-Pad Characteristics for Main-Shaft Seal Applications. NASA TN D-6384, 1971.

10. Ludwig, Lawrence P.; Strom, Thomas N.; Allen, Gorden P.; and Johnson, Robert L.: Improving the Performance of Face Contact Seal in Liquid Sodium (400° to 1000° F) by Incorporation of Spiral-Groove Geometry. NASA TN D-3942, 1967.

11. Russell, Terrence E.; Allen, Gorden P.; Ludwig, Lawrence P.; and Johnson, Robert L.: Gas Turbine Face Seal Thermal Deformation and Computer Program for Calculation of Axisymmetric Temperature Field. NASA TN D-5605, 1969.

NASA-Langley, 1971 — 15 E-6312